

SURFACE AGING IN HIGH REPETITION RATE  
SPARK SWITCHES WITH ALUMINUM AND BRASS ELECTRODES

M. T. Glancy and M. F. Rose

Naval Surface Weapons Center  
Dahlgren, Virginia 22448

Abstract

The surface aging of the electrodes of miniature spark switches ( $A/d \sim 50$ ) is explored using commercial dry nitrogen as the working gas. Both brass and aluminum electrodes were investigated for aging characteristics using a constant gas flow rate of  $8 \text{ cm}^3/\text{sec}$ . The gas pressure was varied from 760 torr-5200 torr. The switches were constructed as an integral part of a miniature L-C oscillator which has a ringing frequency of approximately 150 MHz. The aging process was halted at intervals ranging from one to several thousand discharges and the electrode surface examined with a scanning electron microscope.

surface coatings<sup>2,3</sup> and crystallographic orientation<sup>4</sup> on breakdowns in gases. It has been shown that even thin ( $\sim 10^{-7} \text{ cm}$ ) coatings can greatly alter the breakdown characteristics. In systems demanding high average power, surface heating can easily induce chemical reactions between the working gas and electrode material. These reactions alter the switch characteristics by forming brittle compounds which can flake off the metal surface affecting breakdown voltage and jitter.

In our laboratory, we are currently experimenting with small hertzian generators which must operate continuously for long periods of time at pulse repetition rates of 10's of kilohertz. In another paper in this conference by Rose and Glancy<sup>5</sup>, switches were described which were part of a simple oscillator with a ringing frequency of approximately 150 MHz. By employing gas flow, it is possible to operate these devices at high repetition rates (up to 30 kHz) for long periods of time. The total energy expenditure may be hundreds of kilojoules.

It is the purpose of this paper to explore the surface aging phenomenon and wear characteristics of switches of this type.

Experimental Procedure

The basic oscillator has been described by Moran<sup>6</sup>. Our only modification to this design was to provide for symmetric gas flow and removable electrodes.

In Figure 1, the basic oscillator has capacitance ( $C_o$ ) of 433 pf and inductance ( $2L_o$ ) of 4.3 nH. These values correspond to characteristic oscillator impedance of approximately 3 ohms. The oscillator is fitted with a pressure collar and flow system capable of flow rates as high as 80

Introduction

The problems of electrode wear are relevant to many applications involving high-speed switching such as the relay systems used in telecommunications. Previous work in this area has identified several mechanisms which govern the dynamics of the formation and subsequent growth of spark induced damage<sup>1</sup>. In addition, high repetition rate, pulsed power systems are being constructed which employ spark switches that must carry orders of magnitude greater current and energy. These systems may use different gases, electrode materials, gas pressures, and gas flow rates to minimize erosion and resistive losses while maximizing switch lifetimes and maintaining acceptable operating parameters.

Common to all of these devices are the fast transient currents which can produce discharges exhibiting glow and arc characteristics. Several investigators have explored the effect of electrode

Report Documentation Page			Form Approved OMB No. 0704-0188		
<p>Public reporting burden for the collection of information is estimated to average 1 hour per response, including the time for reviewing instructions, searching existing data sources, gathering and maintaining the data needed, and completing and reviewing the collection of information. Send comments regarding this burden estimate or any other aspect of this collection of information, including suggestions for reducing this burden, to Washington Headquarters Services, Directorate for Information Operations and Reports, 1215 Jefferson Davis Highway, Suite 1204, Arlington VA 22202-4302. Respondents should be aware that notwithstanding any other provision of law, no person shall be subject to a penalty for failing to comply with a collection of information if it does not display a currently valid OMB control number.</p>					
1. REPORT DATE <b>JUN 1979</b>	2. REPORT TYPE <b>N/A</b>	3. DATES COVERED <b>-</b>			
<b>4. TITLE AND SUBTITLE</b> <b>Surface Aging In High Repetition Rate Spark Switches With Aluminum And Brass Electrodes</b>			5a. CONTRACT NUMBER		
			5b. GRANT NUMBER		
			5c. PROGRAM ELEMENT NUMBER		
<b>6. AUTHOR(S)</b>			5d. PROJECT NUMBER		
			5e. TASK NUMBER		
			5f. WORK UNIT NUMBER		
<b>7. PERFORMING ORGANIZATION NAME(S) AND ADDRESS(ES)</b> <b>Naval Surface Weapons Center Dahlgren, Virginia 22448</b>			8. PERFORMING ORGANIZATION REPORT NUMBER		
<b>9. SPONSORING/MONITORING AGENCY NAME(S) AND ADDRESS(ES)</b>			10. SPONSOR/MONITOR'S ACRONYM(S)		
			11. SPONSOR/MONITOR'S REPORT NUMBER(S)		
<b>12. DISTRIBUTION/AVAILABILITY STATEMENT</b> <b>Approved for public release, distribution unlimited</b>					
<b>13. SUPPLEMENTARY NOTES</b> <b>See also ADM002371. 2013 IEEE Pulsed Power Conference, Digest of Technical Papers 1976-2013, and Abstracts of the 2013 IEEE International Conference on Plasma Science. Held in San Francisco, CA on 16-21 June 2013. U.S. Government or Federal Purpose Rights License</b>					
<b>14. ABSTRACT</b> <b>The surface aging of the electrodes of miniature spark switches (A/d ~ SO) is explored using commercial dry nitrogen as the working gas. Both brass and aluminum electrodes were investigated for aging characteristics using a constant gas flow rate of 8 cm<sup>3</sup>/sec. The gas pressure was varied from 760 tort-5200 torr. The switches were constructed as an integral part of a miniature L-C oscillator which has a ringing frequency of approximately 150 MHz. The aging process was halted at intervals ranging from one to several thousand discharges and the electrode surface examined with a scanning electron microscope.</b>					
<b>15. SUBJECT TERMS</b>					
<b>16. SECURITY CLASSIFICATION OF:</b> a. REPORT      b. ABSTRACT      c. THIS PAGE <b>unclassified</b> <b>unclassified</b> <b>unclassified</b>			<b>17. LIMITATION OF ABSTRACT</b> <b>SAR</b>	<b>18. NUMBER OF PAGES</b> <b>7</b>	<b>19a. NAME OF RESPONSIBLE PERSON</b>

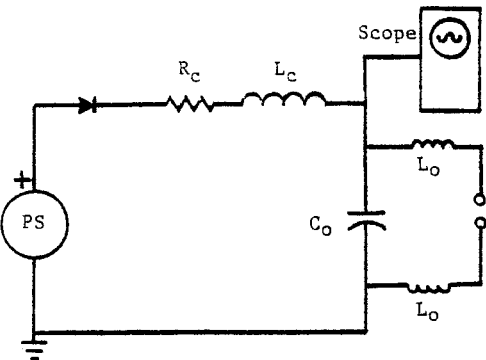


Fig. 1. Schematic of basic charging circuit  
 $\text{cm}^3/\text{sec}$  at pressures as high as  $11.4 \times 10^4$  torr with an absolute accuracy of 50 torr in pressure and flow rates of  $.4 \text{ cm}^3/\text{sec}$ . In the experiments aimed at examining single discharge spots,  $R_c$  was chosen to give a time constant on the order of .2 sec. This value was chosen to allow the gas flow to effectively cool the electrode surface and remove any effects due to gas contamination. A charging choke ( $L_c$ ) was inserted in the charging line to minimize radiation loss at 150 MHz. For these experiments, pressure was varied while maintaining a constant flow rate of  $8 \text{ cm}^3/\text{sec}$ . The oscillator was allowed to run at a low repetition rate until several hundred discharge events occurred.

The experiments to characterize long term wear and surface aging used the same experimental apparatus described by Rose and Glancy<sup>5</sup>. A pulse repetition frequency of 5 khz and a flow rate of  $8 \text{ cm}^3/\text{sec}$  were held constant while pressure was varied.

Figure 2 shows half of the oscillator with those portions marked A and B serving as the electrode and oscillator capacitor respectively. The electrode surfaces were initially levelled on a surface plate with #500 silicon carbide paper and were then mechanically polished using .3 and .05 micron alumina powder. Each portion was given a thorough cleansing in an ultrasonic bath with a final rinse using ethyl alcohol.

Annular dielectric discs were placed between the oscillator halves to determine the system capacitance and gap spacing. A constant spacing of 6

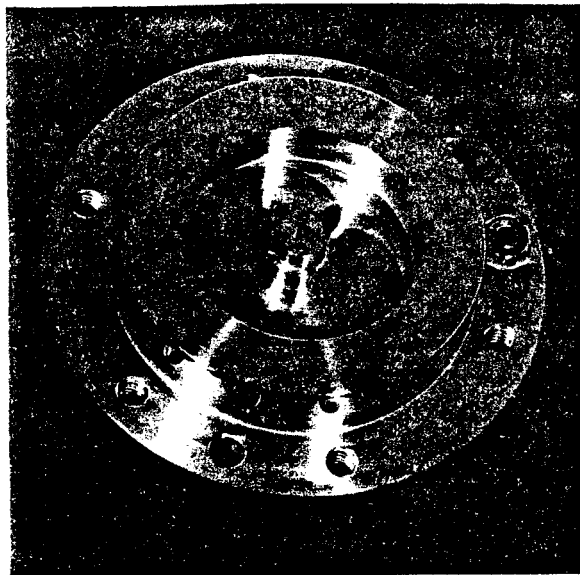


Fig. 2. One-half of the L-C oscillator

mils was used throughout our experiments. Prior to the beginning of each experiment, the system was flushed for several minutes with commercial grade, water-pumped nitrogen gas, which also served as the working gas in the switch.

#### Results and Discussion

After a given experiment, the electrodes were removed and examined for surface damage using an AMR model 1000A electron microscope. The specimen were mounted in the microscope holder in such a way that the beam arrived normal to the surface within a degree or two. The error introduced by specimen tilt was therefore less than the statistical spread in spot diameter. The individual spots appeared reasonably circular with fine structure around the periphery which was pressure and energy dependent.

In each experiment, several hundred spark events were allowed to occur as shown in Figure 3 while simultaneously monitoring the voltage level at which the events occurred. In agreement with the results of Cookson<sup>3</sup> and Coates et al,<sup>7</sup> several discharges occurred before the breakdown voltage reached a relatively constant value. In our analysis, we tended to ignore small spots which we attributed to breakdowns during the initial conditioning portion of the experiment. As can be seen in Figure 3, the spark events occurred at random

on the electrode face which confirmed surface planarity and the statistical nature of the distribution of surface irregularities responsible for breakdown. Individual spots began to coalesce to form a roughened surface as the density of the spots increased.

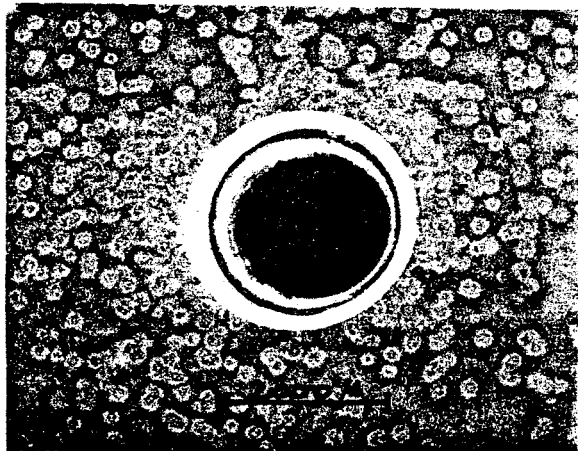


Fig. 3. Overall view of aluminum electrode after spark discharge. Gas pressure  $5.16 \times 10^3$  torr. Large center hole is inlet port for gas.

For both brass (60% Cu, 40% Zn) and aluminum (99.9%) electrodes, we observed three different regions of surface damage which could be attributed directly to a spark discharge. Each individual spot consisted of a central core containing most of the damage as evidenced by surface melting, cratering, and surface flaking. This region was surrounded by a diffuse damage area which was described by Augis et al<sup>8</sup> as the result of a constricted glow discharge. Surrounding these areas, we observed a dark ring which was most likely a product of thermal dissipation in the surface films.

Figure 4 illustrates typical damage from individual discharges, picked from the extrema of our investigations. For both brass and aluminum, the spots shown are on the electrode initially at system ground. The damage on the side initially charged positive was similar and differed mostly in severity. It is obvious from Figure 4 that an individual discharge in aluminum produces more surface damage as indicated by melting, than it does in brass. In addition, the damaged area is larger in brass

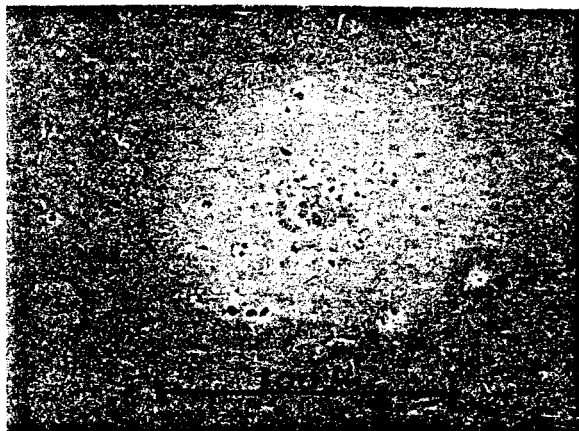
than in aluminum for the same input energy. This is consistent with a higher melting point and lower thermal conductivity for brass.

Table 1. Summary of Data for Brass and Aluminum Electrodes

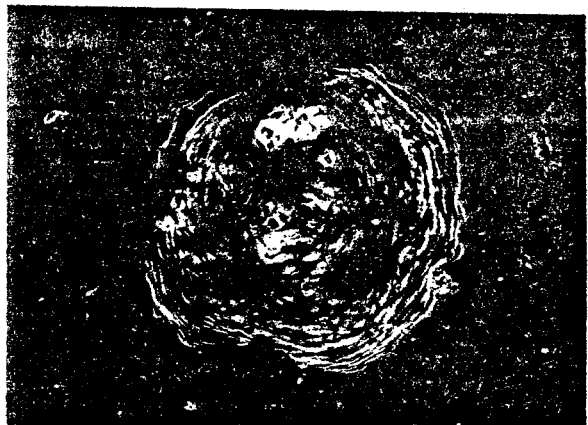
Pressure Torr $\times 10^3$	Voltage kV	Energy mJ	Damage Area $\text{cm}^2 \times 10^{-5}$	
			+	gnd
<b>CuZn</b>				
.76	1.4	.42	4.61	3.23
1.29	2.5	1.35	10.50	9.98
2.58	3.4	2.50	12.80	14.10
3.87	3.8	3.13	16.50	16.60
5.16	4.8	4.99	17.40	27.60
<b>Al</b>				
.76	1.4	.42	3.76	2.15
1.29	2.3	1.15	7.87	8.84
2.58	3.0	1.94	15.55	10.86
3.87	4.1	3.55	14.81	11.40
5.16	5.1	5.52	21.02	17.18

Table 1 summarizes the effects of pressure and the energy in the discharge on the damage area. This area was taken to be the area of a circle whose boundary enclosed all portions of the central core region, including filamentary traces. As the pressure in the gap was raised, the energy associated with the discharge increased with a corresponding increase in spot area.

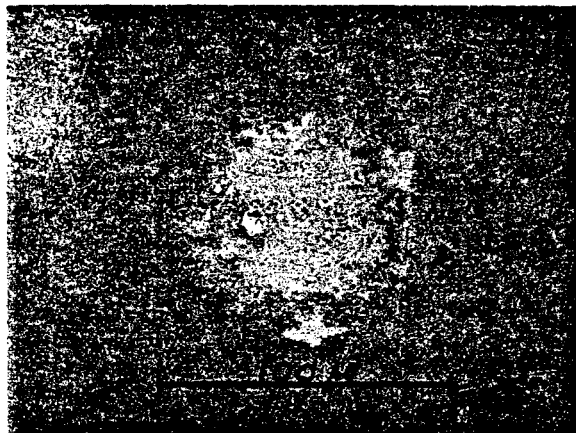
The surface of both electrode materials contained debris which spectroscopic analysis revealed to be various mixtures of the parent metal. The x-ray analyzer on the microscope was incapable of detecting elements with atomic numbers less than twelve; hence, we were unable to determine the exact composition of the debris. However, some of the particles exhibited evidence of surface charging in the electron beam which is typical of insulating materials. Because the gas composition was approximately 99.9% N<sub>2</sub>, we infer that these particles were brittle metal nitrides which flaked off in the flowing gas stream. The formation of such particles is illustrated in Figure 5. Figure 5c shows a magnified portion of a debris field on a "fully aged" electrode surface. Both angular (insulating)



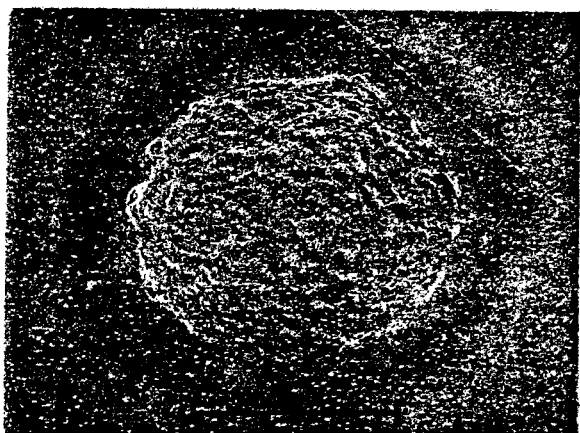
A.



B.



C.



D.

Figure 4. Typical discharge spots show the effect of pressure on spot size and damage.

Electrode initially at system ground.

- A. Aluminum  $7.6 \times 10^2$  torr
- C. Brass  $7.6 \times 10^2$  torr

- B. Aluminum  $5.16 \times 10^3$  torr
- D. Brass  $5.16 \times 10^3$  torr

and globular (pure metal) particles can be seen.

If the device is allowed to run for thousands of shots, the individual discharge spots coalesce. To examine this phenomenon, we ran samples in the assembly described by Rose and Glancy<sup>5</sup> using the experimental parameters described previously. These parameters permitted roughly 5 discharges to occur before the gas was swept from the switch. For short times, individual spots could be distinguished and were similar to those in Figure 3. As the number of discharges increase, spots merge to form a mottled surface, beginning first near the outer rim of the electrode surface and moving

progressively inward as the running time increases. This is consistent with the idea that hot gas and debris, flowing outward from discharges near the center, enhanced the probability of breakdown towards the periphery.

Figure 6 illustrates in both brass and aluminum the surface details of long term aging under flow. For these photographs, the pressure was one atmosphere. Similar structure was observed for higher pressures with differences only in the degree of damage.

The area to the right in Figure 6a is the area immediately beneath the flow inlet on the opposite

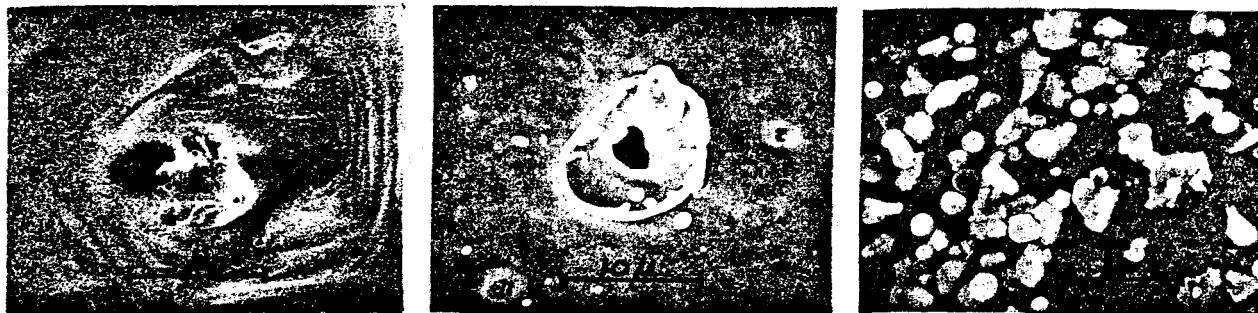


Fig. 5. Views showing flaky mechanism responsible in part for electrode wear.

- A. Interior of a discharge spot aluminum
- B. Interior of a discharge spot brass
- C. Debris field after aging brass

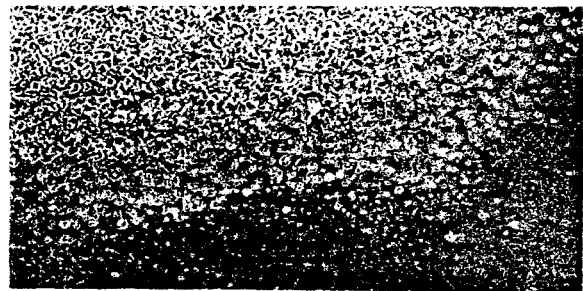
electrode. As one moves out along a radial, the discharge density increases until individual events are no longer discernable. Figure 6b is a higher magnification photo of the transition region between single spots and the eroded outer portion. This region is also characterized by considerable debris of the type shown in Figure 5. Figure 6c and 6d illustrate in detail the heavily worn region. Surface melting and further erosion by both metallic particles and compounds is obvious. Due to extreme temperatures evident in Figure 6, x-ray emission spectroscopy was used to determine the chemical composition in various regions along the surface. For reasons mentioned previous, the analysis is confined to elements greater than atomic number 12. In Figure 6a (brass) the intensity of the emitted x-rays, in the area beneath the flow outlet, associated with the copper and zinc, was in the ratio of 1000:500. A separate scan on a piece of the initial material confirmed this to be the intensity ratio of the brass as received. In the transition region shown in 6b, the intensity ratio changed to 1000:700 indicating a substantial increase in zinc. In the heavy wear region, the intensity ratio was 1000:350 indicating a depletion of zinc. In the region along the electrode periphery the intensity ratio returned to 1000:700 indicating zinc rich. The migration of zinc out of the system was confirmed using color photography. Free copper could be seen on the surface in the heavily damaged region. The boiling points of

copper and zinc are  $2840^{\circ}\text{K}$  and  $1180^{\circ}\text{K}$ . The melting point of brass is  $1173^{\circ}\text{K}$ . While it is impossible in our experiment to obtain a direct measurement of the temperature gradient near the electrode surface, others<sup>9</sup> have estimated the surface temperatures to be as high as  $6000^{\circ}\text{K}$  in similar experiments. It is therefore reasonable for the two constituents to separate, due to the lower boiling point of zinc, and for zinc to migrate to the cooler regions of the electrode which are obviously in the transition region and along the outer rim. Similar scans of aluminum failed to reveal anything but aluminum due to the purity of the material involved.

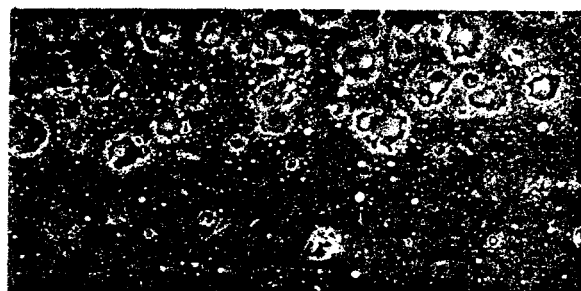
A surface profilometer scan is shown in Figure 7. The surfaces appeared remarkably uniform and showed surface irregularities on the order of 1 mil even though hundreds of kilojoules of energy were dissipated in the gap. The scan was measured about a line joining the center region to a point on the periphery at a similar elevation. A scan such as this presents only surface topography.

#### Summary

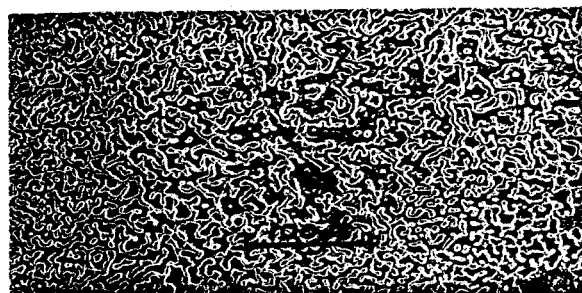
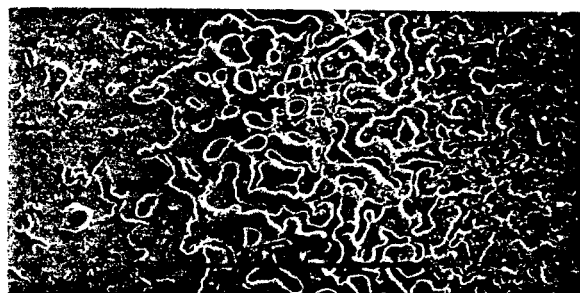
We have examined the surface aging characteristics of spark switches operated at an intermediate repetition rate and under gas flow. The damage produced by individual discharges was found to be a strong function of pressure and energy. As the number of discharges increased, the spots coalesced to form a mottled surface with irregularities on



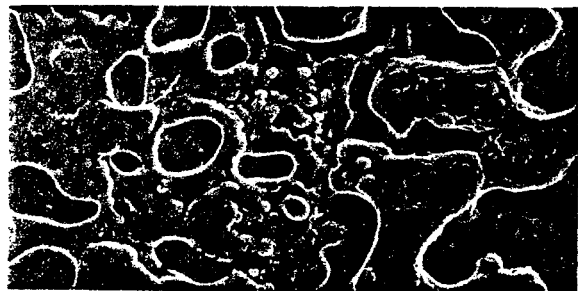
A.



B.



C.



B R A S S



D. A L U M I N U M

Fig. 6. Electrode surface characteristics in brass and aluminum aged for 20 min. at a pressure of  $.76 \times 10^3$  torr. A. Overall view B. Higher magnification showing transition region C. Area in which most of the discharges occurred D. High magnification photograph of the discharge area showing details of surface melting and erosion.

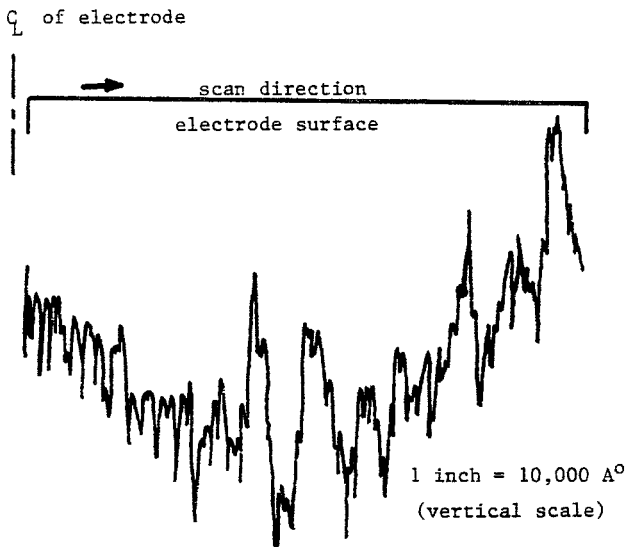


Fig. 7. Profile of brass electrode surface after aging for 30 minutes at a pressure of  $2.58 \times 10^{-3}$  torr.

the order of 10% of the gap spacing. The primary erosion mechanisms were the formation of metal nitrides and metal particles a few microns in diameter. The erosion characteristics for brass are distinctly different than those for aluminum due to thermal induced separation of the constituents.

#### Acknowledgement

This work was sponsored in part by the Defense Advanced Research Projects Agency through the Naval Air Systems Command. In addition we wish to thank Dr. M. K. Norr and C. E. Comford for their assistance during the course of these experiments.

#### References

1. E. W. Gray, "On the Electrode Damage and Current Densities of Carbon Arcs", IEEE Transactions on Plasma Science, Vol. P5-6, pp. 384-393, Dec. 1978.
2. F. L. Jones and C. G. Moran, "Surface Films Field Emission of Electrons", Proc. Roy. Soc., A, 218, pp. 88-103, 1953.
3. A. H. Cookson, "Electrical Breakdown for Uniform Fields in Compressed Gases", Proc. IEE, Vol. 117, p. 269-280, Jan. 1970.
4. Y. L. Stankevick and V. G. Kalinin, "Effect of Cathode Surface State on the Dielectric Strength of Gases and Liquids", Soviet Phys.-Technical Physics, Vol. 14, pp. 949-954, Jan. 1970.
5. M. F. Rose and M. T. Glancy, "High Repetition Rate Miniature Triggered Spark Switch", Proceedings of the Second IEEE International Pulsed Power Conference, 1979.
6. S. L. Moran, "High Repetition Rate L-C Oscillator", IEEE Conference Record of Thirteenth Pulsed Power Modulator Symposium, pp. 254-259, 1978.
7. R. Coates, J. Dutton, P. M. Harris, "Electrical Breakdown of Nitrogen at High Electric Fields", Proc. IEEE, Vol. 125, pp. 158-162, June 1978.
8. J. A. Augis, F. J. Gibson, and E. W. Gray, "Plasma and Electrode Interactions in Short Gap Discharges in Air: Electrode Effects", Int. J. Electronics, Vol. 4, pp. 315-332, 1971.
9. A. E. Guile, "Arc-Electrode Phenomena", Proc. IEE, IEE Reviews, Vol. 118, p. 1132, Sept. 1971.